Human Molecular Genetics, 2011, Vol. 20, No. 22 ***4345–4359***
doi:10.1093/hmg/ddr362
Advance Access published on August 16, 2011

Elevated levels of active matrix metalloproteinase-9 cause hypertrophy in skeletal muscle of normal and dystrophin-deficient mdx mice

Saurabh Dahiya[1], Shephali Bhatnagar[1], Sajedah M. Hindi[1], Chunhui Jiang[2], Pradyut K. Paul[1], Shihuan Kuang[2] and Ashok Kumar[1,*]

[1]Department of Anatomical Sciences and Neurobiology, University of Louisville School of Medicine, Louisville, KY 40202, USA and [2]Department of Animal Sciences, Purdue University, West Lafayette, IN, USA

Received July 12, 2011; Revised July 12, 2011; Accepted August 11, 2011

Matrix metalloproteinases (MMPs) are a group of extracellular proteases involved in tissue remodeling in several physiological and pathophysiological conditions. While increased expression of MMPs (especially MMP-9) has been observed in skeletal muscle in numerous conditions, their physiological significance remains less-well understood. By generating novel skeletal muscle-specific transgenic (Tg) mice expressing constitutively active mutant of MMP-9 (i.e. MMP-9G100L), in this study, we have investigated the effects of elevated levels of MMP-9 on skeletal muscle structure and function *in vivo*. Tg expression of enzymatically active MMP-9 protein significantly increased skeletal muscle fiber cross-section area, levels of contractile proteins and force production in isometric contractions. MMP-9 stimulated the activation of the Akt signaling pathway in Tg mice. Moreover, expression of active MMP-9 increased the proportion of fast-type fiber in soleus muscle of mice. Overexpression of MMP-9 also considerably reduced the deposition of collagens I and IV in skeletal muscle *in vivo*. In one-year-old *mdx* mice (a model for Duchenne muscular dystrophy, DMD), deletion of the *Mmp9* gene reduced fiber hypertrophy and phosphorylation of Akt and p38 mitogen-activated protein kinase. Collectively, our study suggests that elevated levels of active MMP-9 protein cause hypertrophy in skeletal muscle and that the modulation of MMP-9 levels may have therapeutic value in various muscular disorders including DMD.

INTRODUCTION

Skeletal muscle has enormous plasticity to adapt to a wide variety of environmental stimuli. The extracellular matrix (ECM) of skeletal muscle is critical to maintaining its structural integrity, plasticity and normal function (1,2). The role of ECM in skeletal muscle plasticity is evident by the findings that the majority of genes up-regulated in response to exercise training are related to ECM (3). Furthermore, excessive degradation of ECM is a major pathological feature in skeletal muscle degenerative disorders such as muscular dystrophy and inflammatory myopathies (4–7).

Extracellular proteases play a pivotal role in altering local microenvironment during embryonic development and growth and tissue remodeling processes. Matrix metalloproteinases (MMPs) are a relatively large family of Zn^{2+} containing, Ca^{2+}-requiring endopeptidases causing proteolysis of selective ECM components (7,8). MMP-2 (gelatinase A) and MMP-9 (gelatinase B) are the main MMPs that degrade type IV collagen, the most prevalent protein in skeletal muscle basal lamina (9). Despite their similarity in substrate specificity, the general patterns of expression and transcriptional regulation of MMP-2 and MMP-9 are quite different and they appear to regulate different biological processes (9,10). MMP-2 is constitutively expressed by many cell types including skeletal muscle, and its activity has little regulation at the transcriptional level (7,8). In contrast, MMP-9 shows none to minimal basal expression in skeletal muscle (7). However, the transcription of MMP-9 can be highly induced by numerous agents including growth factors,

*To whom correspondence should be addressed at: Department of Anatomical Sciences and Neurobiology, University of Louisville School of Medicine, 500 South Preston Street, Louisville, KY 40202, USA. Tel: +1 5028521133; Fax: +1 5028526228; Email: ashok.kumar@louisville.edu

cytokines, cell–cell and cell–ECM adhesion molecules and agents altering cell shape (11). Elevated levels of MMP-9 have been observed in skeletal muscle in response to physical exercise (12–14) and also in the settings of nerve injury, heart failure and immobilization (15–22). However, the physiological significance of elevated levels of enzymatically active MMP-9 in normal skeletal muscle *in vivo* has not been yet evaluated.

Like other members of this family, MMP-9 is secreted as an inactive proenzyme that can be activated by the removal of the propeptide domain by proteolysis (8,23,24). The latency of MMP-9 is preserved by a cysteine switch mechanism that works through the formation of an intra-molecular complex between the single cysteine residue present in a highly conserved region of the propeptide and the essential zinc atom in the catalytic domain, thereby blocking the active site (25). This cysteine is located within an auto-inhibitory region of the propeptide (consensus sequence PRCGVPDL) of MMPs. However, it has been found that the cysteine switch is not exclusively responsible for maintaining enzyme in latent form. Additional motifs located within the propeptide are necessary to stabilize the propeptide conformation that blocks the active site (26–28). *In vivo*, extracellular activation of these MMPs is typically a result of a two-step process. There is an initial cleavage by an activator protease in an exposed loop of the propeptide domain that destabilizes propeptide binding interactions and disrupts the zinc coordination. This is followed by the second cleavage, generally by an MMP, releasing the mature/active enzyme (7,8). Because of this tight regulation of enzyme activity, it is difficult to mimic the potential active enzyme that might be a part of a physiological or pathological process. Overexpression of MMP-9 would invariably result in increased expression of the latent enzyme but not necessarily increase its activity. Fisher *et al*. (29) made several mutations in the conserved auto-inhibitory region of MMP-9 propeptide to destabilize the interactions responsible for maintaining enzyme latency, bypassing the initial extracellular activation step, resulting in direct expression of active enzyme. It was found that changing glycine residue at position 100 with leucine (G100 → L) in MMP-9 propeptide, auto-catalytically removes the pro-domain, yielding an active enzyme (29). The MMP-9G100L mutant has been successfully used in many studies to evaluate the role and mechanisms of action of active MMP-9 in biological responses (29–31).

Our group and others have previously reported that the levels of MMP-9 are also significantly increased in dystrophin-deficient mdx mice (a mouse model of Duchenne muscular dystrophy, DMD) (18,32). We have also recently reported that the inhibition of MMP-9 alleviates muscle pathology in young (8–10 weeks) mdx mice (32). However, it remains unknown whether inhibition of MMP-9 will also be effective in reducing muscle pathology in aged mdx mice. Furthermore, the mechanisms of action of MMP-9 in dystrophic muscle remain poorly understood.

The major goal of the present study was to investigate the role of increased levels of enzymatically active MMP-9 protein in skeletal muscle. To this end, we have generated transgenic (Tg) mice over-expressing MMP-9G100L mutant in skeletal muscle. Our study showed that elevated levels of MMP-9 in skeletal muscle leads to hypertrophy, improves strength, diminishes collagen deposition and causes transition of slow-type fibers into fast type. Moreover, our experiments have revealed that the genetic ablation of MMP-9 diminishes muscle injury and fiber hypertrophy in diaphragm of 1-year-old mdx mice.

RESULTS

Generation of skeletal muscle-specific MMP-9G100L Tg mice

Skeletal muscle-specific Tg mice expressing MMP-9G100L protein were generated by expressing MMP9G100L cDNA under the control of muscle creatine kinase (MCK) promoter. The design of the Tg construct is described in Figure 1A. To validate that this construct produces active MMP-9 protein, C2C12 myoblasts were transfected with vector alone (i.e. pCCLMCKII plasmid), wild-type (WT) MMP-9 or increasing amounts of pCCLMCKII-MMP-9G100L plasmid, and the cells were differentiated into myotubes by incubation in differentiation medium for 96 h. Finally, the cells were incubated in serum-free medium for 24 h and the culture supernatants collected were analyzed by gelatin zymography and western blot. Transfection of pCCLMCKII-MMP-9G100L plasmid dose-dependently increased the amounts of both pro and active forms of MMP-9 in culture supernatants (Fig. 1B). In contrast, transfection with WT MMP-9 cDNA increased the expression of only pro-MMP-9 in culture supernatants (Fig. 1B). Upon confirming that pCCLMCKII-MMP-9G100L construct produces active MMP-9 protein, the expression cassette was isolated by digesting pCCLMCKII-MMP-9G100L plasmid with *Swa*I enzyme and purified DNA was used for pronuclear injections. Genotyping of founder mice using tail DNA confirmed the presence of transgene in several mice (Fig. 1C). Finally, colonies of the founder mice were established and two independent colonies stably expressing MMP-9G100L protein in skeletal muscle were utilized for the present study. Tg mice expressed elevated levels of both pro- and active forms of MMP-9 protein in their skeletal muscle evaluated by gelatin zymography and western blotting (Fig. 1D). Immunostaining of muscle sections using anti-MMP-9 and anti-laminin confirmed that the expression of MMP-9 was increased around sarcolemma and cytoplasm of muscle fibers of MMP-9G100L Tg mice (Fig. 1E).

To understand the effects of over-expression of active MMP-9 protein in skeletal muscle of mice, we first measured body weight and individual muscle weight. There was no significant difference in body weight between WT and MMP-9G100L Tg mice till the age of 3 months. However, at the age of 6 and 9 months, body weight of MMP-9G100L Tg was significantly high compared with littermate WT mice (Supplementary Material, Fig. S1A). Similarly, gross weight of soleus (Supplementary Material, Fig. S1B) and tibial anterior (TA) muscle (data not shown) was significantly higher in MMP-9G100L Tg mice compared with WT mice at the age of 6 and 9 months. Measurement of serum levels of creatine kinase (CK) did not show any significant difference between MMP-9G100L Tg and littermate WT mice analyzed at the age of 8 months (data not shown). Similarly, there was

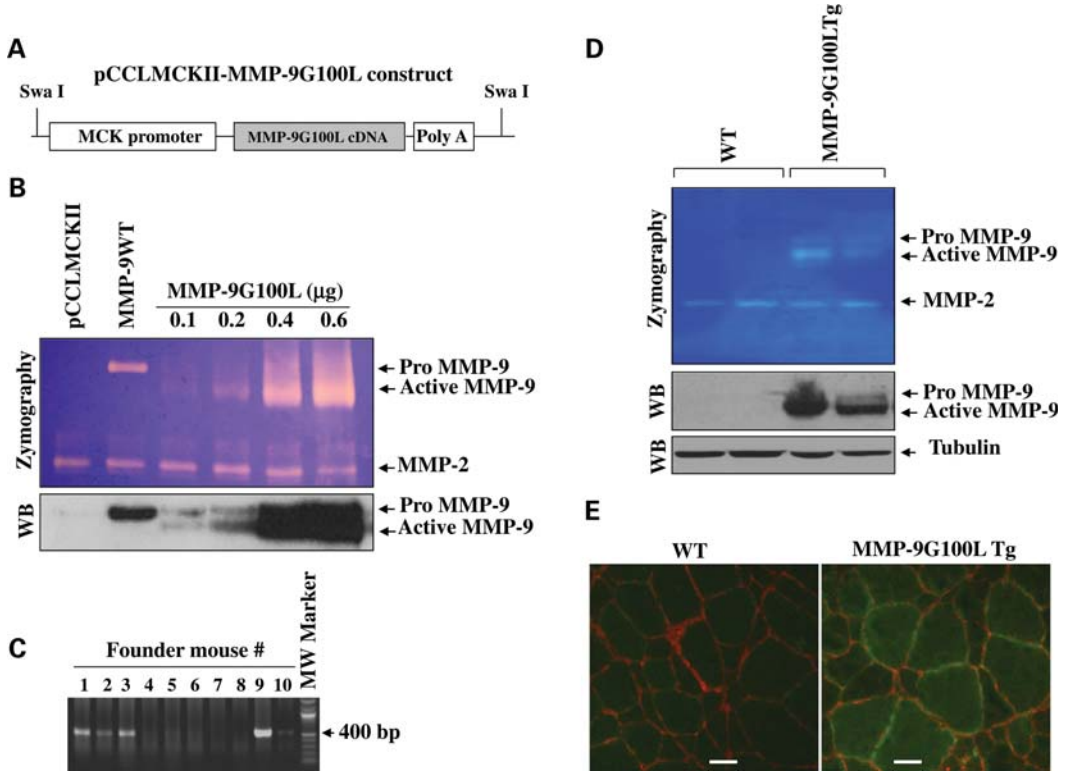

Figure 1. Generation of MMP-9G100L Tg mice. (**A**) Design of the construct used for generation of MMP-9G100L Tg mice. (**B**). C2C12 myoblasts plated in six-well tissue culture plate were transfected with vector alone, WT MMP-9 or indicated amounts of pCCLMCKII-MMP-9G100L plasmid. Cells were differentiated into myotubes and levels of MMP-9 in culture supernatants were measured by gelatin zymography and western blot (WB). Representative photomicrographs of zymography and immunoblot gels are presented here. (**C**) Agarose gel run after polymerase chain reaction (PCR) showing presence of transgene in founder mouse # 1, 2, 3 and 9. (**D**) TA muscle extracts prepared from two independent colonies (lines #1 and 9) of MMP-9G100L Tg mice and littermate WT mice were analyzed by zymography and western blotting. Data presented here show expression of active MMP-9 protein in muscle of MMP-9G100L Tg mice. (**E**) Double immunostaining of muscle sections prepared from TA muscle of 3 months old of WT and MMP-9G100L Tg mice using anti-MMP-9 and anti-laminin. Scale bar: 20 μm.

no significant difference in mRNA levels of proinflammatory cytokines tumor necrosis factor-α and interleukin-1β between WT and MMP-9G100L Tg mice (data not shown) indicating that overexpression of MMP-9G100L protein does not cause any overt muscle pathology or inflammation.

Tg expression of MMP-9G100L protein causes hypertrophy in skeletal muscle

To understand the effects of increased levels of active MMP-9 protein on skeletal muscle structure *in vivo*, we isolated TA and soleus muscle from 4- and 8-month-old MMP-9G100L Tg and littermate WT mice. Frozen transverse sections made from mid belly of these muscles were stained with hematoxylin and eosin (H&E). Skeletal muscle from MMP-9G100L-Tg mice was morphologically similar to littermate WT mice both at the age of 4 months (Supplementary Material, Fig. S1C) and 8 months (Fig. 2A). While quantitative estimation of fiber cross-sectional area (CSA) showed no significant difference between WT and MMP-9G100L mice at the age of 4 months (Supplementary Material, Fig. S1C), the average fiber CSA was significantly higher in soleus and TA muscle of MMP-9G100L Tg mice compared with littermate WT mice (Fig. 2B). Furthermore, there were a few fibers (∼2%) which showed central nucleation both at the age of 4 months (Supplementary Material, Fig. S1C) and 8 months (Fig. 2A). As a complementary approach to study the effects of overexpression of MMP-9G100L on skeletal muscle, we cultured single myofiber from extensor digitorum longus (EDL) muscle of 8-month-old WT and MMP-9G100L Tg mice (Fig. 2C and D) and quantified their diameter. Interestingly, average diameter of cultured myofibers was significantly higher in MMP-9G100L Tg mice compared with WT mice (Fig. 2D).

Elevated levels of MMP-9G100L promote muscle regeneration and growth

Since MMP-9G100L Tg mice showed hypertrophy and a few centrally nucleated myofibers, we next sought to determine whether elevated levels of MMP-9 increased muscle formation or regeneration in Tg mice. We measured the mRNA levels of muscle-specific transcription factors myogenin and MyoD, which are co-expressed during skeletal muscle growth/regeneration (33). Interestingly, mRNA levels of MyoD and myogenin were significantly higher in TA muscle of MMP-9G100L Tg mice compared with littermate WT mice (Fig. 3A).

Satellite cells are the muscle progenitor cells which are required not only for muscle development but also for

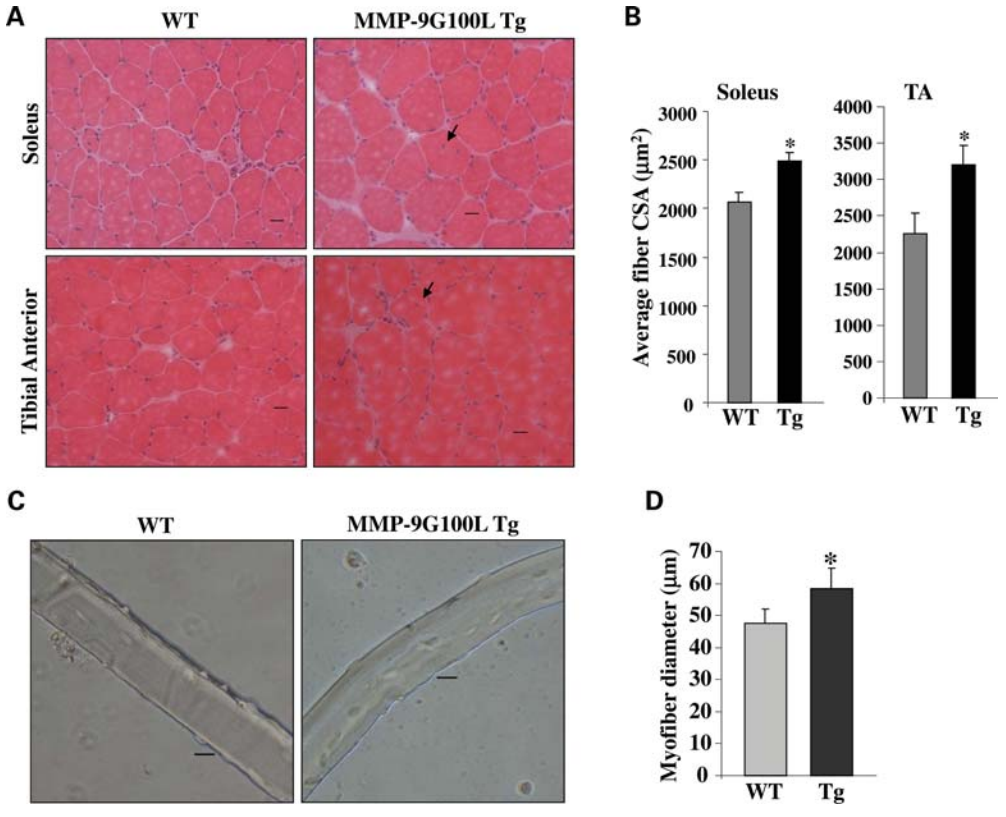

Figure 2. Increased fiber CSA in skeletal muscle of MMP-9G100L Tg mice. Soleus and TA muscle were isolated from 8-month-old littermate WT and MMP-9G100L Tg mice and transverse muscle section made were stained with H&E dyes. (**A**) Representative H&E-stained pictures of soleus and TA muscle of WT and MMP-9G100L Tg mice. Arrows point to central nucleation. Scale bar: 20 μm. (**B**) Quantification of average fiber CSA in H&E-stained sections of littermate WT and MMP-9G100L Tg mice. $N = 6$ in each group. (**C**) Representative photomicrographs of single myofibers prepared from EDL muscle of 8-month-old WT and MMP-9G100L Tg mice. Scale bar: 20 μm. (**D**) Quantitative estimation of mean diameter of myofibers. $^{*}P < 0.05$, values significantly different from WT mice. Error bars represent SD.

regeneration of adult myofibers after injury and for post-natal muscle growth (33). We next sought to determine whether MMP-9G100L protein affects the number of myofiber-associated satellite cells *in vivo*. Previous studies have shown that a unique combination of cell surface markers ($CD45^{-}$, $CD31^{-}$, $Ter119^{-}$, $\alpha7\text{-}\beta1$ $integrin^{+}$) identify satellite cells in adult mouse skeletal muscle and allow their direct quantification and/or isolation by fluorescence-activated cell sorting (FACS) technique (34). Though a slight increase in number of satellite cells was observed in skeletal muscle of MMP-9G100L Tg mice (Fig. 3B), it was not significantly different from that of WT mice (Fig. 3B and C). We also quantified number of satellite cells in single myofibers isolated from EDL muscle of WT and MMP-9G100L Tg mice. Immunostaining of myofibers using Pax-7 and 4′,6-diamidino-2-phenylindole (DAPI) showed the presence of Pax-7-positive nuclei (Fig. 3D). However, there was no significant difference in the number of Pax-7-positive cells per fiber between WT and MMP-9G100L Tg mice (Fig. 3E).

We further investigated whether MMP-9G100L protein affects the proliferation and differentiation of satellite cells *in vitro.* Primary myoblasts/satellite cells were isolated from TA muscle of littermate WT and MMP-9G100L Tg mice. Proliferation of cultured myoblasts was studied by monitoring cell division and colony formation. As shown in Supplementary Material, Figure S2, there was no significant difference in the proliferation of cultured myoblasts between WT and MMP-9G100L Tg mice. Interestingly, when the cultured myoblasts were allowed to differentiate into myotubes by incubation in differentiation medium, a significant increase in myotube formation was noticeable in MMP-9G100L Tg cultures compared with WT mice (Supplementary Material, Fig. S3A). Number of nuclei per myotube and average myotube diameter were significantly higher in MMP-9G100L Tg compared with WT cultures, measured 5 days after induction of differentiation (Supplementary Material, Fig. S3B and C). These results suggest that the increased levels of MMP-9 promote fusion of myoblasts into myotubes.

To further establish the role of MMP-9 in skeletal muscle regeneration *in vivo*, we also studied skeletal muscle regeneration in WT and MMP-9G100L Tg mice in response to cardiotoxin-induced injury. Since skeletal muscle of young WT and MMP-9G100L Tg mice do not show any structural difference or hypertrophy, we used 8-week-old mice for this experiment. As shown in Supplementary Material, Figure S4A, the regeneration of TA muscle was significantly improved in MMP-9G100L Tg mice compared with WT mice measured after 5 or 10 days of cardiotoxin injection.

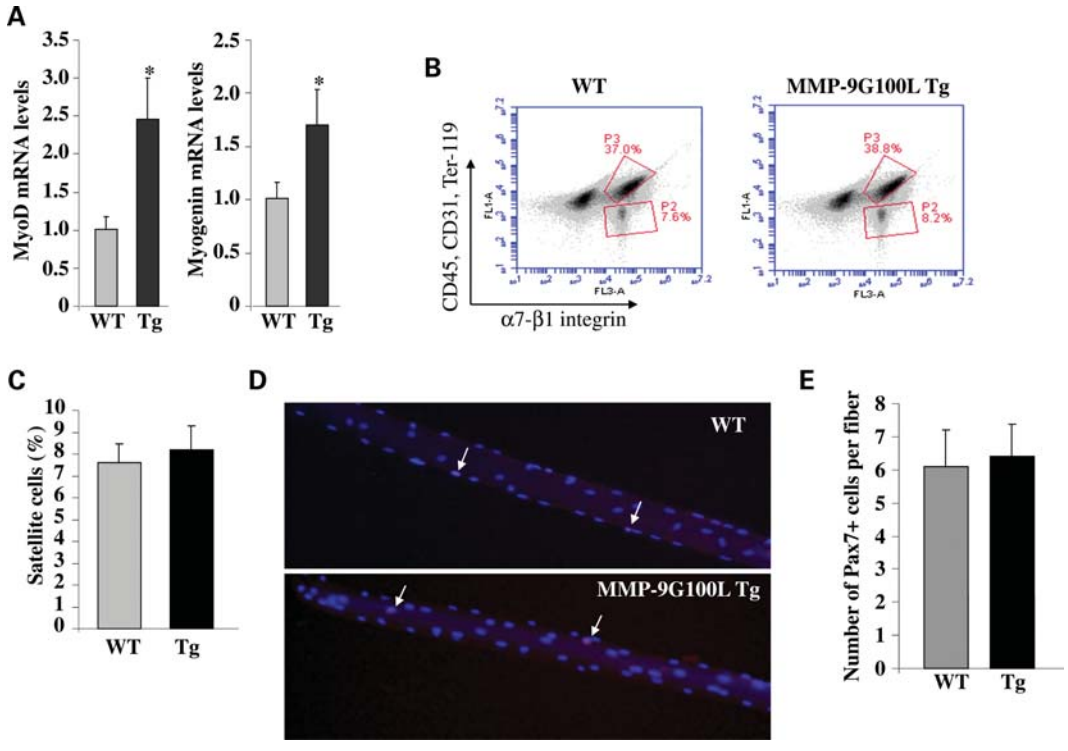

Figure 3. Expression of myogenic regulatory factors and quantification of number of satellite cells in skeletal muscle of WT and MMP-9G100L Tg mice. (**A**) TA muscle was isolated from 8-month-old WT and MMP-9G100L Tg mice and processed for total RNA isolation and measurement of mRNA levels of MyoD and myogenin by QRT-PCR technique. $N = 4$ in each group. (**B**) Flow cytometric analysis (FACS) of satellite cells in WT and MMP-9G100L Tg mice. Mononuclear cells were isolated from TA and gastrocnemius muscle of WT and MMP-9G100L mice. Following appropriate immunostaining, the cells were analyzed by flow cytometry. Representative results of analysis of isolated mononuclear cells are presented here. P2 box represents the percentage of satellite cells. (**C**) Quantitative estimation of number of satellite cells from WT and MMP-9G100L Tg mice. $N = 4$ in each group. (**D**) Representative pictures of single fibers stained with Pax-7 antibody and DAPI. Arrows point to Pax-7-positive nuclei. (**E**) Quantification of number of Pax-7-positive cells per fiber from WT and MMP-9G100L Tg mice. $^{*}P < 0.05$, values significantly different from WT mice. Error bars represent SD.

Quantitative estimation of fiber CSA in regenerating myofibers 10 days after cardiotoxin injection also supported the inference that MMP-9G100L protein promotes skeletal muscle regeneration *in vivo* (Supplementary Material, Fig. S4B). Collectively, these results suggest that MMP-9 does not affect proliferation but promotes fusion of muscle progenitor cells leading to enhanced muscle formation and growth.

Levels of contractile proteins are increased in skeletal muscle of MMP-9G100L-Tg mice

At the molecular level, skeletal muscle hypertrophy is characterized by increased levels of several thick and thin filament proteins (35,36). To further evaluate the effects of overexpression of MMP-9G100L protein in skeletal muscle, we measured the levels of a select few proteins in TA muscle of WT and MMP-9G100L Tg mice by western blotting. The levels of thick filament protein, myosin heavy chain (MyHC) and thin filament proteins, tropomyosin and troponin were substantially increased in TA muscle of MMP-9G100L Tg mice compared with littermate WT mice (Fig. 4A and B). Furthermore, protein levels of laminin and neuronal nitric oxide synthase (nNOS) were also significantly higher in TA muscle of MMP-9G100L Tg mice compared with WT mice. Elevated levels of MMPs can cause proteolytic degradation of cytoskeletal protein β-dystroglycan (30,37,38). We performed western blotting to determine whether increased expression of MMP-9G100L protein reduces the levels of β-dystroglycan in skeletal muscle. Surprisingly, we did not find any significant difference in the levels of β-dystroglycan protein in TA muscle of control and MMP-9G100L Tg mice (Fig. 4A and B).

Accumulating evidence suggests that skeletal muscle mass and fiber hypertrophy can be regulated by the presence of a number of growth modulators (39,40). Myostatin is a negative regulator of skeletal muscle mass (40). In contrast, insulin growth factors (IGFs) and follistatin positively regulate skeletal muscle regeneration and growth (40,41). We next investigated whether the overexpression of MMP-9G100L protein affects the expression of any of these molecules in skeletal muscle *in vivo*. Interestingly, while MMP-9G100L did not affect the transcript levels of myostatin, it augmented the expression of both IGF-I and follistatin in skeletal muscle of Tg mice (Fig. 4C). The increased expression of IGF-I and follistatin could be one of the potential reasons for observed hypertrophy and improved muscle regeneration in MMP-9G100L Tg mice.

Activation of phosphatidylinositol-3 kinase/Akt signaling pathway in skeletal muscle of MMP-9G100L Tg mice

Akt (also known as protein kinase B) is a central kinase of phosphatidylinositol-3 kinase (PI3K)/Akt signaling pathway,

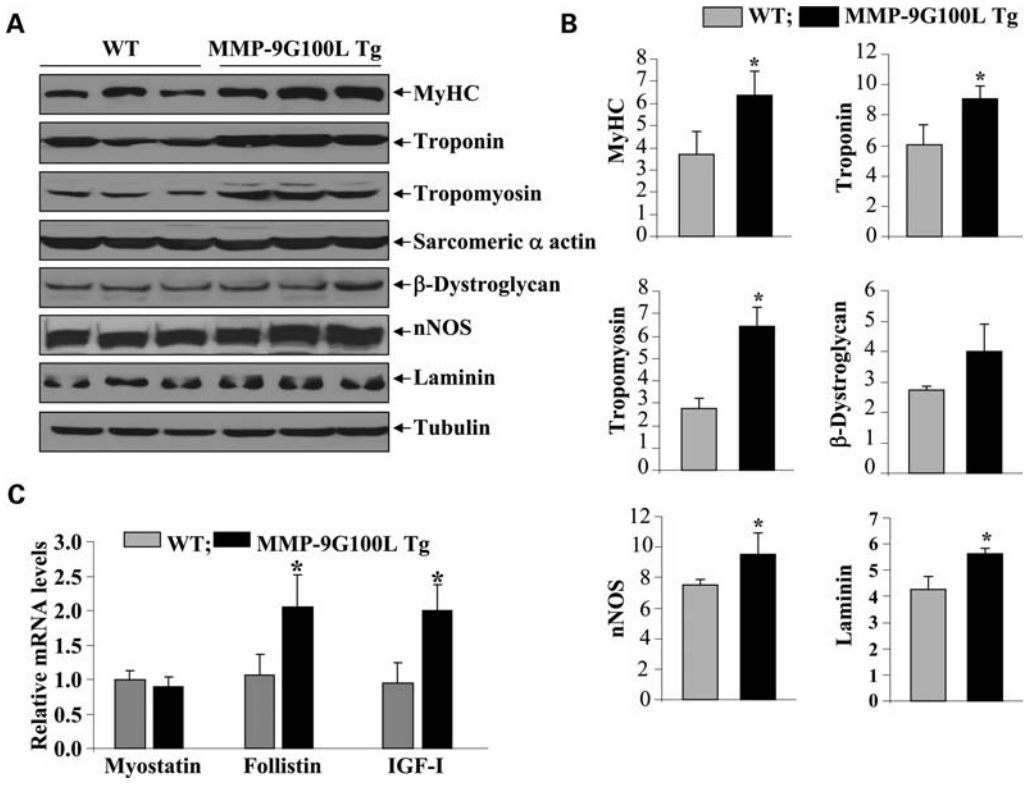

Figure 4. Levels of specific muscle protein in skeletal muscle of WT and MMP-9G100L Tg mice. (**A**) Protein extracts prepared from TA muscle of 8-month-old littermate WT and MMP-9G100L Tg mice were immunoblotted with antibody against MyHC, troponin, tropomyosin, sarcomeric α actin, β-dystroglycan, nNOS, laminin and an unrelated protein tubulin. Representative immunoblots are shown here. (**B**) Densitometry quantification of immunoblots of WT and MMP-9G100L Tg mice. $N = 6$ in each group. (**C**) Relative mRNA levels of myostatin, IGF-I and follistin in TA muscle of 8-month-old WT ($N = 3$) and MMP-9G100L Tg ($N = 4$) mice measured by QRT-PCR technique. $^{*}P < 0.05$, values significantly different from WT mice. Error bars represent SD.

whose activation is strongly linked to protein synthesis and skeletal muscle hypertrophy (35,36,42). We investigated whether overexpression of MMP-9 affects the activation of PI3K/Akt pathway in skeletal muscle of mice. TA muscle extracts prepared from littermate WT and MMP-9G100L Tg mice were used to determine the levels of total and phosphorylated Akt protein by western blot. Interestingly, phosphorylation of Akt protein was significantly increased in skeletal muscle of MMP-9G100L Tg mice compared with WT mice (Fig. 5A). Moreover, the levels of phosphorylation of mammalian target of rapamycin (mTOR) and FOXO1, the downstream phosphorylation targets of Akt (42), were also found to be significantly increased in Tg mice compared with WT mice (Fig. 5A and C).

In addition to Akt kinase, several other signaling proteins, especially mitogen-activated protein kinases (MAPKs), have been implicated in skeletal muscle remodeling in the conditions of hypertrophy and/or atrophy (39). We next investigated whether MMP-9G100L protein affects the activation of MAPK in skeletal muscle of Tg mice. We performed western blot using antibody that detects phosphorylated form of specific MAPKs. As shown in Figure 5B, there was no significant difference in the levels of phosphorylation of extracellular-regulated kinase 1/2 (ERK1/2) and c-Jun N-terminal kinase 1/2 (JNK1/2). However, the phosphorylation of p38 MAPK was found to be significantly reduced in skeletal muscle of MMP9-G100L Tg mice compared with WT littermates (Fig. 5B and C).

MMP-9 causes transition of slow-type oxidative fibers into fast-type glycolytic fibers

One of the unique features of skeletal muscle is its composition of different muscle fiber types, and its ability to switch fiber type to meet particular physiological demands (43). Since soleus muscle contains both slow- and fast-type fibers, we investigated whether the expression of MMP-9G100L protein affects the composition of oxidative (type I, slow-type) and glycolytic (type II, fast-type) fibers in mice. Staining of soleus muscle section for MyHC type I, IIA and IIB protein (Fig. 6) followed by counting each type of fiber revealed that the soleus muscle of MMP-9G100L Tg mice contained significantly increased number of fast-type and reduced number of slow-type fibers compared with littermate WT mice (Fig. 6D). Specifically, type IIB fibers that were not detectable in WT soleus muscle emerged in the MMP-9G100L Tg soleus muscle (Fig. 6C). However, we did not find any significant difference in fiber-type composition in TA muscle (data not shown) which could be attributed to the fact that TA muscle of mice contains predominantly fast-type fibers.

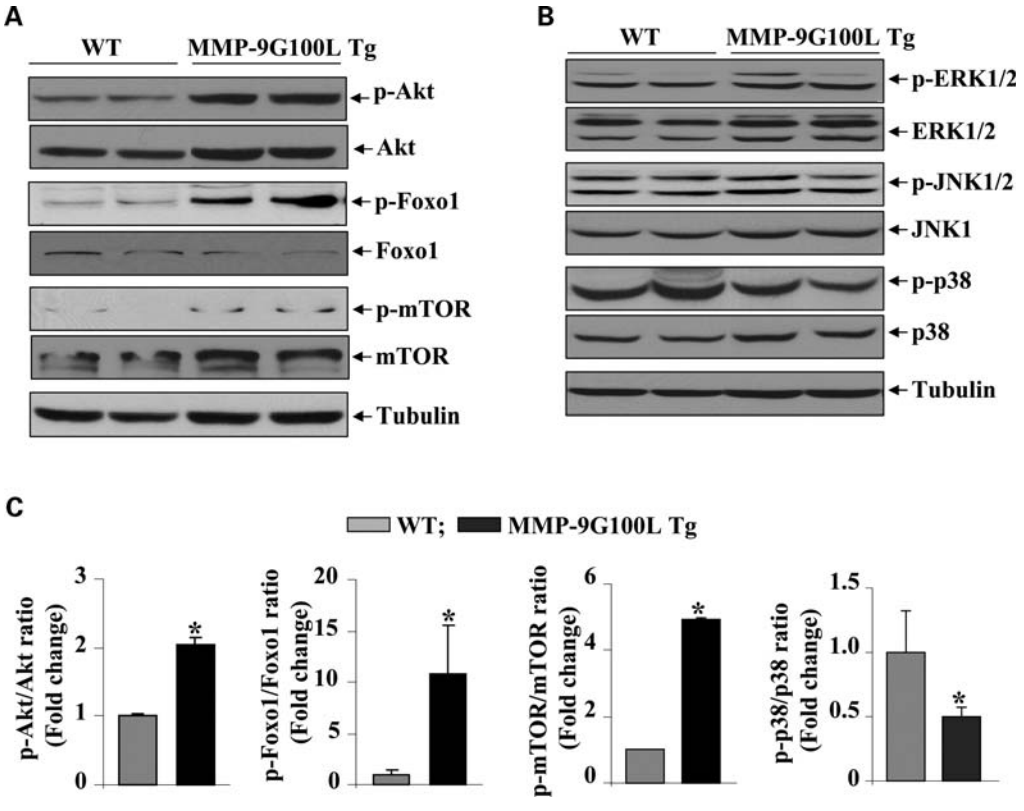

Figure 5. Activation of PI3K/Akt/mTOR pathway in skeletal of MMP-9G100L Tg mice. Muscle extracts prepared from TA muscle of 8-month-old WT and MMP-9G100L Tg were immunoblotted with antibody that detects phosphorylated or total levels of indicated protein. (**A**) Representative immunoblots are shown here. (**B**) Immunoblotting of muscle extracts using antibody against phospho-ERK1/2, phospho-JNK1/2 and phospho-p38 MAPK showed no significant difference between WT and MMP-9G100L Tg mice. (**C**) Densitometric quantification of immunoblots. $N = 4$ in each group. $^{*}P < 0.05$, values significantly different from WT mice. Error bars represent SD.

Tg expression of MMP-9G100L protein diminishes accumulation of collagens and improves skeletal muscle contractile function in mice

We next sought to determine the effect of overexpression of MMP-9G100L protein on development of interstitial fibrosis in skeletal muscle. Though skeletal muscle may contain many types of collagens, collagen I, III and IV are the major components of ECM in skeletal muscle (1). By performing immunostaining, we first investigated whether elevated levels of active MMP-9 protein affects the levels of collagens I, III and IV in skeletal muscle of Tg mice. As shown in Figure 7A, levels of collagens I and IV were found to be reduced in TA muscle of MMP-9G100L Tg mice compared with littermate WT mice. In contrast, there was no difference in the levels of collagen III in TA muscle of WT and MMP-9G100L Tg mice. Western blot analyses further confirmed that protein levels of collagens I and IV (but not collagen III) were considerably reduced in TA muscle of MMP-9G100L Tg mice compared with WT littermates (Fig. 7B).

We also studied the effects of overexpression of MMP-9G100L protein on soleus muscle force production in isometric contractions. Consistent with hypertrophic phenotype and increased number of fast-type fibers, specific force production in isometric contractions was significantly higher in soleus muscle of MMP-9G100L Tg mice compared with littermate WT mice at all the frequencies studied (Fig. 7C).

Genetic ablation of MMP-9 reduces serum levels of CK and fiber hypertrophy in 1-year-old mdx mice

The dystrophin-deficient mdx mice serve as a model of DMD (44). These mice are phenotypically normal at birth but undergo cycles of fiber degeneration and regeneration starting at 2.5 weeks of age (44). Similar to human DMD patients, the diaphragm in the older *mdx* mice shows significant increases in muscle fiber loss, fibrosis, inflammatory cell invasion and fiber hypertrophy (45–47). We have previously reported increased levels of MMP-9 in 7–10-week-old mdx mice and that inhibition of MMP-9 improves several pathological features in skeletal muscle in these mice (32). However, it is not known whether the levels of MMP-9 remained elevated in older mdx mice and whether the inhibition of MMP-9 will also be effective in improving muscle pathology in diaphragm of aged mdx mice. Western blotting showed that the protein levels of MMP-9 are significantly elevated in diaphragm of 1-year-old mdx/Mmp9$^{+/+}$ mice compared with littermate WT mice (Fig. 8A). MMP-9 protein was undetectable in diaphragm of mdx/Mmp9$^{-/-}$ mice (Fig. 8A). We next measured the serum levels of CK, a marker of muscle injury, in 1-year-old mdx/Mmp9$^{+/+}$, and mdx/Mmp9$^{-/-}$ mice. CK levels were significantly reduced in mdx/Mmp9$^{-/-}$ mice compared with mdx/Mmp9$^{+/+}$ mice, suggesting that ablation of MMP-9 reduces overall muscle injury in mdx mice (Fig. 8B). We also performed H&E staining on transverse

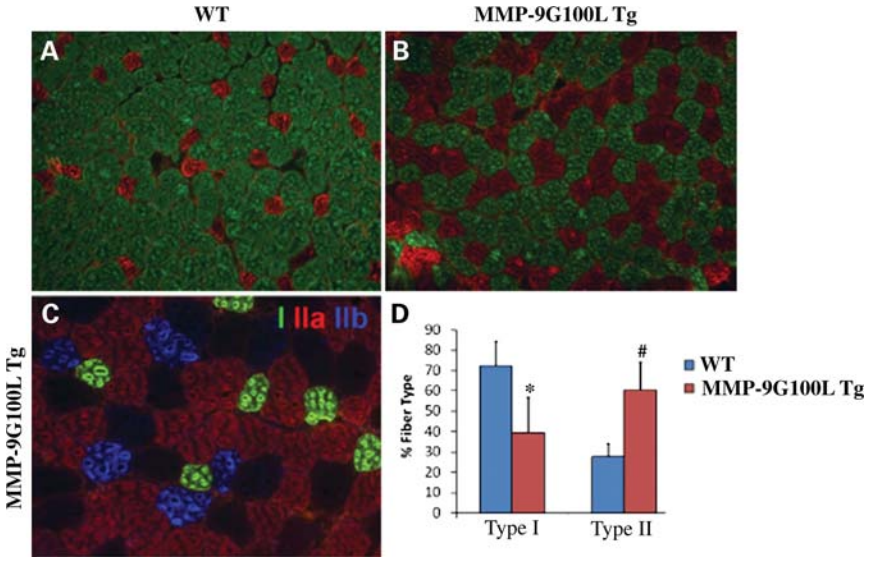

Figure 6. MMP-9G100L promotes transformation of slow-type fibers into fast-type in Tg mice. Soleus muscle sections prepared from WT and MMP-9G100L Tg mice were subjected to triple immunostaining against MyHC I, IIA and IIB protein. (**A**) Soleus muscle of WT mice showed mostly type I slow fibers (green). (**B**) Overexpression of MMP-9G100L protein increased the number type IIA fibers (red). (**C**) Higher magnification of soleus muscle section of MMP-9G100L Tg mice showing emergence of IIB (blue) and IIx (black) fibers that are not seen in soleus muscle of WT mice. Quantification of type I and type II fibers in WT ($N = 6$) and MMP-9G100L Tg ($N = 5$) mice. $^{*}P < 0.05$, values significantly different from WT mice. Error bars represent SD. $^{\#}P < 0.01$, values significantly different from WT mice.

sections prepared from diaphragm of WT, mdx/Mmp9$^{+/+}$ and mdx/Mmp9$^{-/-}$ mice. As shown in Figure 8C, the diaphragm of mdx/Mmp9$^{+/+}$ mice showed fibers with variable size, hypertrophy, centronucleated fibers (CNF) and cellular infiltrate, the typical features of dystrophic muscle (46,48,49). In contrast, fiber size was considerably reduced in diaphragm of mdx/Mmp9$^{-/-}$ mice although it still contained some cellular infiltrate and CNF (Fig. 8C). Quantitative estimation of fiber cross-section area (CSA) of fibers (having CSA $>500\ \mu m^2$) confirmed that fiber hypertrophy is significantly reduced in mdx/Mmp9$^{-/-}$ compared with mdx/Mmp9$^{+/+}$ mice (Fig. 8D). Moreover, the variability in fiber CSA (Fig. 8E) and the number of centronucleated myofibers (Fig. 8F) were also significantly reduced in diaphragm of mdx/Mmp9$^{-/-}$ mice compared with mdx/Mmp9$^{+/+}$ mice.

Genetic ablation of MMP-9 reduces phosphorylation of Akt and p38 MAPK in diaphragm of mdx mice

Since the activation of Akt pathway is increased in myofibers of MMP-9G100L Tg mice and there are published reports that Akt activity is up-regulated in myofibers of mdx mice (50–52), we next sought to determine whether genetic ablation of MMP-9 affects the phosphorylation of Akt kinase in mdx mice. Protein extracts prepared from diaphragm of 1-year-old WT, mdx/Mmp9$^{+/+}$ and mdx/Mmp9$^{-/-}$ mice were immunoblotted using antibody that detects phosphorylated or total Akt protein. As shown in Figure 9, the phosphorylation of Akt kinase was significantly reduced in mdx/Mmp9$^{-/-}$ mice compared with mdx/Mmp9$^{+/+}$ mice. We further investigated whether MMP-9 affects the activation of MAPKs in diaphragm of mdx mice. Interestingly, the phosphorylation of p38MAPK was significantly reduced in mdx/Mmp9$^{-/-}$ mice compared with mdx/Mmp9$^{+/+}$ mice (Fig. 9A and B). However, there was no significant difference between the level of phosphorylation of ERK1/2 or JNK1/2 between mdx/Mmp9$^{+/+}$ and mdx/Mmp9$^{-/-}$ mice (Fig. 9A).

DISCUSSION

In the past decade, several reports have been published demonstrating increased expression/activation of various MMPs including MMP-9 in skeletal muscle in diverse conditions (7,10,12–14,17). However, the physiological significance of elevated levels of MMP-9 in skeletal muscle remained enigmatic. To understand the role of increased activity of MMP-9 in skeletal muscle, we engineered novel Tg mice expressing an enzymatically active MMP-9 mutant using MCK promoter, which ensures increased levels of MMP-9, predominantly in skeletal muscle (Fig. 1).

Because of the suggested role of MMP-9 in tissue destruction in many disease states, we anticipated that overexpression of active MMP-9 mutant in skeletal muscle of mice would cause severe myopathy. However, contrary to this presumption, our experiments showed that the increased levels of active MMP-9 cause hypertrophy, increase proportion of fast-type glycolytic fibers and improve muscle contractile function *in vivo*. Interestingly, the results of the present study are consistent with a recently published study by Mehan *et al*. (53) where they reported a reduction in fiber CSA and altered fiber-type composition in skeletal muscle of female *Mmp9*-null mice compared with corresponding WT mice.

It has been consistently observed that resistance exercise augments the levels of MMPs, including MMP-9, in skeletal muscle of both human and animal models (12–14), indicating that MMP-9 might be involved in skeletal muscle remodeling

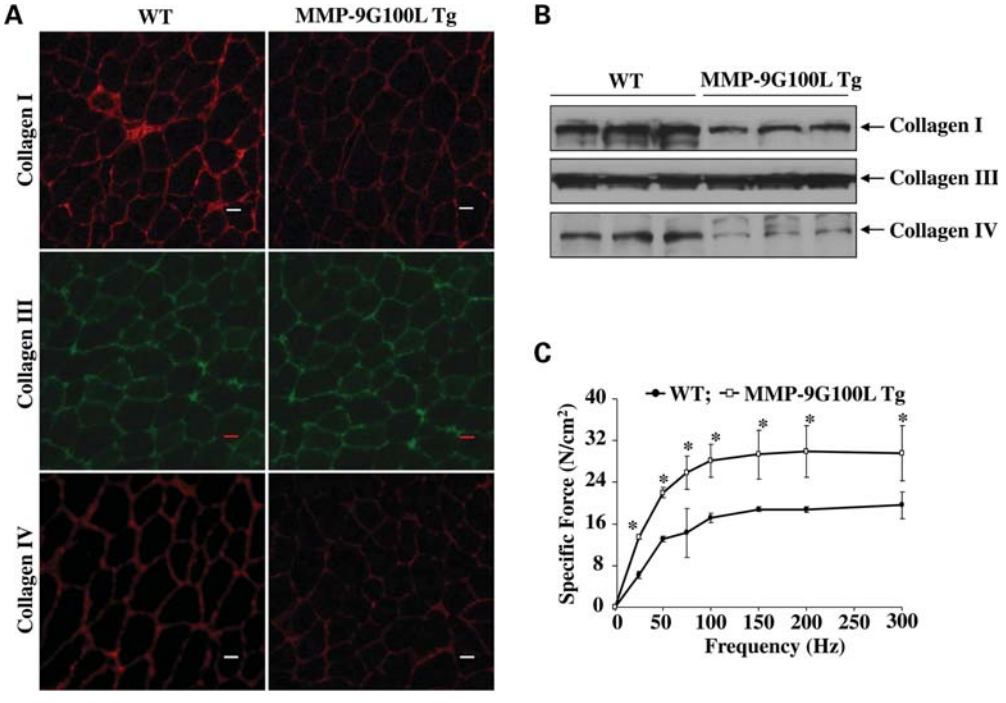

Figure 7. Effect of Tg overexpression of MMP-9G100L protein on expression of collagens and muscle function. (**A**) TA muscle isolated from 8-month-old WT and MMP-9G100L Tg mice were subjected to immunostaining for collagen I, III or IV. Representative photomicrographs presented here demonstrate that the protein levels of collagens I and IV but not collagen III are considerably reduced in MMP-9G100L Tg mice compared with WT mice. (**B**) Western blot analysis of collagen I, III and IV proteins in TA muscle of 8-month-old WT and MMP-9G100L Tg mice. $N = 3$ in each group. (**C**) Force-frequency curves. Data presented here are the average force produced by soleus muscle of WT ($N = 4$) and MMP-9G100L Tg mice ($N = 4$). $^{*}P < 0.05$, values significantly different from MMP-9G100L Tg mice at corresponding frequency. Error bars represent SD.

leading to fiber hypertrophy in exercised muscle. Indeed, it has been previously suggested that resistance exercise causes minor trauma to skeletal muscle which initiates the proliferation of satellite cells and their fusion with mature myofibers resulting in hypertrophy (54–56). While we found a few CNF, we did not find any sign of inflammation or other muscular abnormalities in MMP-9G100L Tg mice (Fig. 2A). Therefore, it is possible that the increased levels of active MMP-9 might be causing some injury to muscle fibers and in the absence of pathological stimuli, this injury leads to increased fusion of satellite cells with mature myofibers resulting in muscle growth. It is noteworthy that MMP-9 is one of the most important extracellular proteases, which can cleave collagen IV and laminin present in basement membrane and hence can cause sarcolemmal damage (24).

MyoD and myogenin are the two most important muscle-specific transcription factors involved in expression of several contractile proteins in skeletal muscle (57–59). The expression of both MyoD and myogenin is generally increased in response to resistance exercise and/or during muscle regeneration after injury (33,60). Our data demonstrating increased levels of MyoD and myogenin (Fig. 3A) and the presence of a few CNF (Fig. 2A) are suggestive of enhanced muscle growth and/or regeneration in MMP-9G100L Tg mice. While the exact mechanisms remain unknown, it is possible that the increased levels of MMP-9 facilitate the migration and eventual fusion of satellite cells with adult myofibers. This possibility is supported by our cell culture experiments where the number of nuclei per myotube and average myotube diameter were significantly increased in MMP-9G100L Tg cultures after addition of differentiation medium (Supplementary Material, Fig. S3). Furthermore, enhanced regeneration of TA muscle in MMP-9G100L Tg mice after cardiotoxin injury is indicative of the possibility that MMP-9 promotes skeletal muscle growth/hypertrophy *in vivo* potentially through augmenting the efficiency of satellite cells to fuse with injured myofibers.

Several published reports suggest that the activation of the PI3K/Akt/mTOR signaling pathway can enhance protein synthesis in skeletal muscle resulting in hypertrophy (36,42,61). More recent studies have shown that the activation of this pathway inhibits skeletal muscle atrophy by inhibiting the activity of Foxo family of transcription factors, which regulates the expression of specific 'atrogenes' in skeletal muscle (36,62,63). The increased phosphorylation of Akt and mTOR and the elevated levels of several muscle proteins (e.g. MyHC, tropomyosin, troponin and nNOS) observed in skeletal muscle of MMP-9G100L Tg mice indicate that one of the mechanisms by which MMP-9 might be causing hypertrophy is through augmenting the activity of PI3K/Akt/mTOR pathway. Moreover, increased phosphorylation of Foxo1 transcription factor (leading to its reduced activity) in myofibers of MMP-9G100L Tg mice may also reduce basal protein turnover resulting in increased protein content in skeletal muscle (Fig. 5A and B). How elevated levels of MMP-9 stimulate PI3K/Akt/mTOR pathway in skeletal muscle remains enigmatic? Since MMP-9 is known to affect the expression as well as activation of various latent growth factors, cytokines

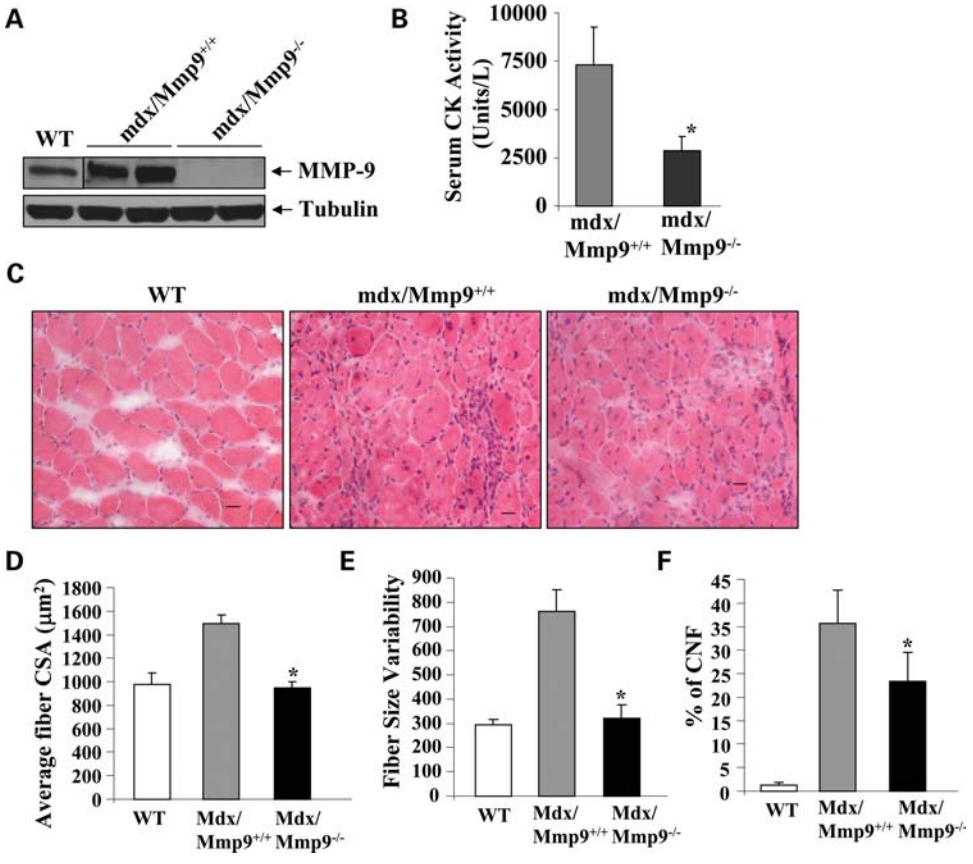

Figure 8. Ablation of MMP-9 reduces muscle injury and hypertrophy in 1-year-old mdx mice. (A) Protein extracts prepared from diaphragm of 1-year-old WT, mdx/Mmp9$^{+/+}$ and mdx/Mmp9$^{-/-}$ mice analyzed by western blot using MMP-9 antibody. Representative immunoblot presented here demonstrates increased levels of MMP-9 in diaphragm of mdx/Mmp9$^{+/+}$ mice compared with WT mice. MMP-9 protein was undetectable in mdx/MMP-9$^{-/-}$ mice. (**B**) Plasma levels of CK were significantly reduced in 1-year-old mdx/Mmp9$^{-/-}$ mice compared with littermate mdx/Mmp9$^{+/+}$ mice. (**C**) Frozen transverse sections of diaphragm from 1-year-old WT, mdx/Mmp9$^{+/+}$ and mdx/Mmp9$^{-/-}$ mice were stained with H&E and photomicrographed. Scale bar: 20 μm. Data presented here demonstrate that the deletion of the *Mmp9* gene in mdx mice reduces muscle hypertrophy and variability in fiber size. (**D**) Quantification of average fiber CSA from H&E-stained sections of WT, mdx/Mmp9$^{+/+}$ and mdx/Mmp9$^{-/-}$ mice. (**E**) Variability in fiber size is significantly reduced in diaphragm of mdx/Mmp9$^{-/-}$ mice compared with littermate mdx/mmp9$^{+/+}$ mice. (**F**) Quantification of CNF in diaphragm of WT, mdx/Mmp9$^{+/+}$ and mdx/mmp9$^{-/-}$ mice. $^{*}P < 0.05$, values significantly different from WT mice. Error bars represent SD.

and matrix proteins (24,64), it is possible that MMP-9 augments the levels of specific growth factors, which in turn bind to their specific cell surface receptors on muscle fibers, leading to the activation of PI3K/Akt/mTOR pathway and hence hypertrophy. Indeed, our experiments have provided initial evidence that the expression levels of growth stimulatory molecules IGF-I and follistatin are significantly elevated in skeletal muscle of MMP-9G100L Tg mice (Fig. 4C). Interestingly, both IGF-I and follistatin are the potent activators of PI3K/Akt/mTOR signaling pathway in skeletal muscle (40,41).

We have also found that the age-related collagen deposition is considerably reduced in skeletal muscle of MMP-9G100L Tg mice compared with WT mice (Fig. 7A and B). These results are somewhat in contrast to published reports which suggest that the elevated levels of MMP-9 exacerbate fibrosis in other tissues in different disease models (32,65), although there is also evidence that overexpression of MMP-9 reduces fibrosis (66). However, it is important to note that in disease conditions, in addition to MMP-9, the levels of many other MMPs, cytokines and inflammatory cells are also simultaneously upregulated which may collectively induce fibrosis. In the present study, we used mice which express only MMP-9 and the muscle tissues were otherwise healthy. These results suggest that the presence of active MMP-9 in ECM induces collagen metabolism leading to reduced accumulation of fibrotic tissues in skeletal muscle which is also consistent with published reports that MMP-9 can degrade multiple collagens including collagens I, IV, III and V present in skeletal muscle tissues (24,64). Reduced levels of fibrosis may also be responsible for an increase in force production observed in soleus muscle of MMP-9G100L Tg mice compared with WT mice (Fig. 7C). Moreover, accumulation of fibrotic tissues in ECM may also diminish the availability of growth factors and migration of satellite cells (67). Thus, declined levels of fibrosis upon expression of enzymatically active MMP-9 protein may also induce hypertrophy by augmenting the bioavailability of certain growth factors and migration of satellite cells providing another potential mechanism for increased muscle hypertrophy in MMP-9G100L Tg mice. Alternatively, there is a possibility that elevated levels of MMP-9 augment the degradation of

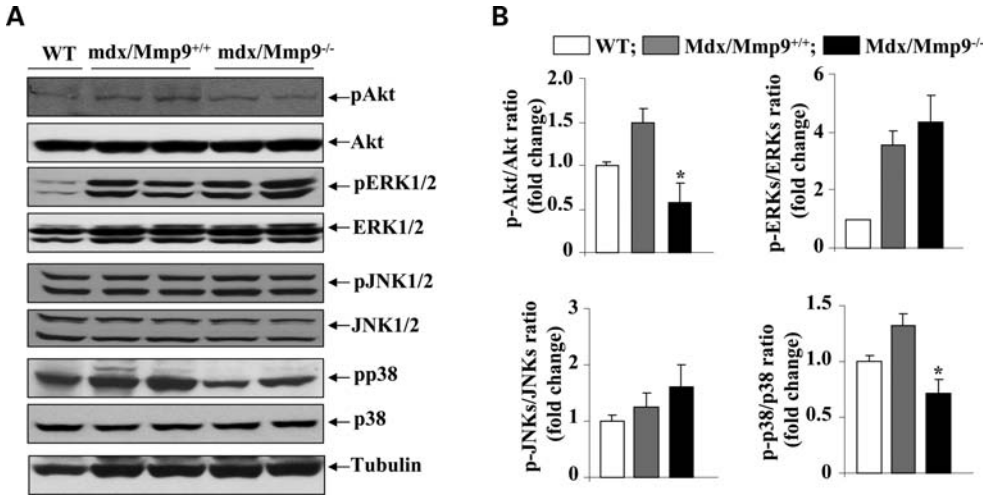

Figure 9. Effects of genetic ablation of MMP-9 on the activation of Akt and MAPKs in diaphragm of 1-year-old mdx mice. (**A**) Protein extracts prepared from diaphragm of 1-year-old WT, mdx/Mmp9$^{+/+}$ and mdx/Mmp9$^{-/-}$ mice were immunoblotted using antibody against phosphorylated or total Akt, ERK1/2, JNK1/2 and p38MAPK. Representative immunoblots presented here show that the level of phosphorylation of Akt and p38MAPK was reduced in diaphragm of mdx/mmp9$^{-/-}$ mice compared with mdx/Mmp9$^{+/+}$ mice. (**B**) Densitometric quantification of immunoblots. $N = 4$ in each group. $^{*}P < 0.05$, values significantly different from mdx/Mmp9$^{+/+}$ mice. Error bars represent SD.

ECM proteins, thus causing laxation of the restriction by ECM on muscle fiber, resulting in increased fiber growth.

DMD involves breakdown of ECM, fiber degeneration, inflammation and eventually replacement of skeletal muscle tissues with fibrotic tissues (6). Levels of MMP-9 are considerably increased in dystrophic muscle of mdx mice (10,18,32) and we have previously reported that the ablation of MMP-9 improves muscle pathology in young mdx mice (32). Our experiments in this study have shown that the levels of CK in serum remained significantly lower in 1-year-old mdx/Mmp9$^{-/-}$ mice compared with littermate mdx/Mmp9$^{+/+}$ mice (Fig. 8B), indicating that inhibition of MMP-9 reduces muscle injury in aged mdx mice as well. Although genetic evidence regarding the role of p38MAPK in mdx mouse pathology is still lacking, there has been suggestions that the increased activation of p38MAPK and MMPs exacerbate muscle pathology in mdx mice (68,69). Our study demonstrates that the ablation of MMP-9 reduces the phosphorylation of p38MAPK in dystrophic muscle of mdx mice (Fig. 9A). Furthermore, average fiber CSA (Fig. 8D) and the phosphorylation of Akt kinase (Fig. 9A and B) were also considerably reduced in mdx/Mmp9$^{-/-}$ mice compared with mdx/Mmp9$^{+/+}$ mice, suggesting that MMP-9 causes hypertrophy in diaphragm of mdx mice potentially through activation of Akt kinase.

While MMP-9 appears to be involved in inducing fiber hypertrophy it is of considerable importance to note that the pathogenesis of mdx mice is quite complex and MMP-9 could be one of many proteins involved in muscle pathology in mdx mice. This is also somewhat evident from our results demonstrating that while genetic ablation of MMP-9 improved muscle structure in mdx mouse, it did not completely restore muscle architecture (Fig. 8C). On the similar lines, overexpression of MMP-9G100L protein in skeletal muscle did not produce any structural or functional deteriorations or inflammation, which are the prominent pathological features of dystrophic muscle, further suggesting that MMP-9 may not be the sole mediator of myopathy in the settings of muscular dystrophy.

In summary, our study suggests that the increased levels of active MMP-9 protein cause fiber hypertrophy *in vivo*. This study improves our basic understanding of the mechanisms of action of MMP-9 in skeletal muscle. These results may also have important therapeutic implications for development of novel therapies for DMD patients.

MATERIALS AND METHODS

Mice

Control (strain: C57BL10/ScSn), mdx (strain: C57BL/10ScSn DMD^{mdx}) and *Mmp9*-knockout (strain: FVB.Cg-*Mmp9*tm1Tvu) mice were purchased from Jackson Laboratory (Bar Harbor, ME, USA). *Mmp9*-knockout mice were first crossed with C57BL10/ScSn mice for seven generations and then with mdx mice to generate littermate WT, mdx;*Mmp9*$^{+/+}$ and mdx;Mmp9$^{-/-}$ mice as previously described (32). All genotypes were determined by polymerase chain reaction (PCR) analysis from tail DNA. Mice were housed in the animal facility of the University of Louisville under conventional conditions with constant temperature and humidity and fed a standard diet. All experiments with animals were approved by the Institutional Animal Care and Use Committee of the University of Louisville.

MMP-9G100L Tg mice

Skeletal muscle-specific Tg mice were generated following similar method as described previously (70). cDNA encoding auto-activating form of human MMP-9 (i.e. MMP9G100L) as described (31) was kindly provided by Dr Elaine W. Raines of the University of Washington, Seattle. The MMP-9G100L cDNA was ligated at the *Pac*I site in the pCCLMCKII vector (a gift by Dr Ulla M. Wewer). In the pCCLMCKII

vector, the expression of target gene is under the control of MCK promoter, which ensures the expression of target protein predominantly in skeletal muscle. The cDNA encoding MMP-9G100L was ligated at the *Pac*I site in the pCCLMCKII plasmid and the orientation of cDNA was confirmed by DNA sequencing. The expression cassette containing the MCK promoter, MMP-9G100L cDNA and poly(A) tail was excised by *Swa*I restriction enzyme, purified and provided to the Core Transgenic Facility of the University of Cincinnati for injection into the pronucleus of a fertilized ovum. Founder mice obtained were screened for the presence of transgene by PCR using genomic DNA from the tail tip and colonies of Tg mice were established. To study the effects of MMP-9G100L protein on adult muscle regeneration, 100 μl of 10 μmol/l cardiotoxin (CalBiochem) dissolved in phosphate-buffered saline (PBS) was injected into the TA muscle of 8-week-old WT and MMP-9G100L Tg mice to induce necrotic injury. After 5 and 10 days, TA muscle was collected from euthanized mice for histology studies.

Cell culture

C2C12 (a mouse myoblastic cell line) cells were obtained from the American Type Culture Collection (Rockville, MD, USA). The cells were grown in Dulbecco's modified Eagle's medium (DMEM) containing 10% fetal bovine serum (FBS). Cells were transfected with plasmid vectors using Effectene Reagent following manufacturer's instructions (Qiagen, Valencia, CA, USA).

Primary mouse myoblasts were isolated and cultured from hind limb skeletal muscle of mice following a protocol as described (71). In brief, skeletal muscles from mice were aseptically isolated, minced into coarse slurry and enzymatically digested at 37°C for 1 h by adding 200 IU/ml collagenase I (Worthington, cat # LS004196) and 0.1% pronase (EMD Chemicals, cat # 53702). Digested slurry was filtered through a 70 μm filter, and spun and isolated cells were resuspended and cultured initially in F-10 medium (containing 20% FBS and supplemented with 10 ng/ml basic fibroblast growth factor) and then in F-10 plus DMEM (1:1 ratio) based culture medium supplemented with 15% FBS on culture dishes coated with 10% matrigel (BD biosciences). Differentiation in C2C12 or primary myoblast cultures was induced by replacing the growth medium with differentiation medium (2% horse serum in DMEM).

Single muscle fiber culture and staining

For single myofiber isolation, EDL muscle was dissected tendon to tendon from mice and enzymatically digested in DMEM medium supplemented with collagenase (400 IU/ml, Worthington, LS004196) at 37°C for 45 min. Post-digestion, single myofibers were released by trituration in myofiber culture medium (DMEM with 10% FBS). Single myofibers were plated on 10% BD-matrigel (BD biosciences, 354 230) coated dishes and stained for anti-Pax-7 and DAPI following a standard protocol as described (72). Fluorescent-labeled myofibers were visualized on microscope (Eclipse TE 2000-U) using a Plan 10X, NA 0.25 PH1 DL objective lens, respective color-filters, a digital camera (Digital Sight DS-Fi1) and NIS Elements BR 3.00 software (all from Nikon).

FACS analysis

Activated satellite cells were analyzed by FACS as described (34). In brief, satellite cells were isolated from TA muscle of WT and MMP-9G100L Tg following same protocol as described above for myoblast preparation. Approximately 2×10^6 cells were incubated in DMEM (supplemented with 2% FBS and 25 mM 4-(2-hydroxyethyl)-1-piperazineethanesulfonic acid) with antibody against CD45, CD31, Ter119 (eBiosciences) and α7β1-integrin (MBL International) conjugated with phycoerythrin or tandem-PE conjugate, respectively. FACS analysis was performed on a C6 Accuri cytometer equipped with three lasers and CFlow Plus Software.

Histology and morphometric studies

Skeletal muscle tissues were removed, frozen in isopentane cooled in liquid nitrogen and sectioned in a microtome cryostat. For the assessment of tissue morphology, 10 μm thick transverse sections of each muscle were stained with H&E, and staining was visualized on a microscope (Eclipse TE 2000-U), a digital camera (Digital Sight DS-Fi1) and NIS Elements BR 3.00 software (all from Nikon). The images were stored as JPEG files, and image levels were equally adjusted using Photoshop CS2 software (Adobe). Fiber CSA was analyzed in H&E-stained soleus, diaphragm or TA muscle sections. For each muscle, the distribution of fiber CSA was calculated by analyzing 200–250 myofibers using NIS Elements BR 3.00 software (Nikon) as described (73). Variability in CSAs between samples was expressed as the mean of the standard deviations (SD) for each population as described (48,73). Percentage of CNF was determined by counting the number of fibers with nuclei in center divided by total number of fibers in each section.

Muscle fiber-type immunostaining

Cross-sections of soleus and TA muscles were blocked in 5% goat serum and 2% bovine serum albumin for 45 min, and incubated for 1 h with monoclonal antibodies to type I, IIa and IIb MyHC isoforms using clone HB287, HB277 and HB283, respectively (ATCC). Secondary antibody used was goat anti-mouse IgG2b conjugated with Alexa-647, goat anti-mouse IgG1 conjugate with Alexa-568 and goat anti-mouse IgM conjugated with Alexa-488. Fluorescence was captured with a Leica-6000M microscope with green, red and infrared bandpass filters, respectively.

CK assay

The serum level of CK was determined using a commercially available kit (Stanbio Laboratory, TX, USA) as described (32). CK activity was expressed as units/liter.

Western blot

Skeletal muscle tissues were washed with PBS and homogenized in lysis buffer A [50 mM Tris–Cl (pH 8.0), 200 mM NaCl, 50 mM NaF, 1 mM dithiotheritol (DTT), 1 mM sodium orthovanadate, 0.3% IGEPAL, and protease inhibitor cocktail]. Approximately, 100 μg protein was resolved on each lane on 8–12% sodium dodecyl sulfate–polyacrylamide gel electrophoresis (SDS–PAGE), electrotransferred onto nitrocellulose membrane and probed using anti-MMP-9 (1:1000, R&D Systems), MF-20 (1:1000, Development Studies Hybridoma Bank, University of Iowa), anti-laminin (1:1000, Sigma-Aldrich), anti-tropomyosin (1:2000, Sigma-Aldrich), anti-troponin (1:1000, Sigma-Aldrich), anti-sarcomeric α-actin (1:1000, Sigma-Aldrich), anti-nNOS (1:500, Santa Cruz Biotechnology, Inc.), anti-β-dystroglycan (1:500, Santa Cruz), anti-phospho p44/p42 (1:1000, cell Signaling), anti-p44/p42 (1:1000, Cell Signaling, Inc.), anti-phospho-JNK1/2 (1:1000, Cell signaling, Inc.), anti- JNK1/2 (1:1000, Santa Cruz), anti-phospho p38 (1:500, Santa Cruz), anti-p38 (1:1000, Cell Signaling, Inc.), anti-phospho Akt (1:1000, Cell Signaling, Inc.), anti-Akt (1:1000, Cell Signaling, Inc.), anti-phospho Foxo1 (1:1000, Cell Signaling, Inc.), anti-Foxo1 (1:1000, Cell Signaling, Inc.), anti-phospho mTOR (1:500, Cell Signaling, Inc.), anti-mTOR (1:1000, Cell Signaling, Inc.), anti-collagen I (1:1000; Abcam), anti-collagen III (1:1000; Abcam), anti-collagen IV (1:500; Abcam) and anti-tubulin (1:3000, Cell Signaling, Inc.) and detected by chemiluminescence. For collagens I and III detection, muscle extracts were prepared in lysis buffer lacking DTT and separated on SDS–PAGE under non-reducing conditions. To compare relative expression levels of specific protein between mice, western blot band intensity was quantified and values were analyzed. Briefly, western blot bands on X-ray films were scanned to TIFF files at 300 dpi in Adobe PS2; images were converted to 8-bit gray scale and band intensity for each band was quantified using ImageJ software (National Institute of Health, USA). Background was subtracted from each band and adjusted mean peak intensities were used for analysis.

Gelatin zymography

Gelatin zymography was performed following similar protocol as described previously (32).

Quantitative real-time PCR (QRT-PCR)

RNA isolation and quantitative real-time PCR (QRT-PCR) were performed using a method as detailed previously (73).

Skeletal muscle functional studies

Soleus muscle contractile properties were determined following a method as previously described (32). In brief, soleus muscle was rapidly excised and placed in Krebs–Ringer solution. The muscle was mounted between a Fort25 force transducer (World Precision Instrumentation) and a micromanipulator device in a temperature-controlled myobath (World Precision Instrumentation). The muscle was positioned between platinum wire stimulating electrodes and stimulated to contract isometrically using electrical field stimulation (supramaximal voltage, 1.2 ms pulse duration) using a Grass S88 stimulator. In each experiment, muscle length was adjusted to optimize twitch force (optimal length, Lo). The muscle was rested for 30 min before the tetanic protocol was started. The output of the force transducer was recorded in computer using LAB-TRAX-4 software. Maximal tetanic contraction was assessed at 300 Hz for 500 ms duration. To investigate a potentially different frequency response between groups, tetanic contractions were assessed by sequential stimulation at 25, 50, 75, 100, 150, 200 and 300 Hz with 2 min rest in between. The CSA for each muscle was determined by dividing muscle weight by its length and tissue density (1.06 g/l), and muscle force was compared after corrections for CSA.

Statistical analysis

Results are expressed as mean ± SD. Statistical analysis used Student's *t*-test or aalysis of variance to compare quantitative data populations with normal distribution and equal variance. A value of $P < 0.05$ was considered statistically significant unless otherwise specified.

SUPPLEMENTARY MATERIAL

Supplementary Material is available at *HMG* online.

Conflict of Interest statement. None declared.

FUNDING

This work was supported by funding from Muscular Dystrophy Association and National Institute of Health grants AG029623 and AR059810 to A.K.

REFERENCES

1. Kjaer, M. (2004) Role of extracellular matrix in adaptation of tendon and skeletal muscle to mechanical loading. *Physiol. Rev.*, **84**, 649–698.
2. Sanes, J.R. (2003) The basement membrane/basal lamina of skeletal muscle. *J. Biol. Chem.*, **278**, 12601–12604.
3. Pette, D. (2001) Historical perspectives: plasticity of mammalian skeletal muscle. *J. Appl. Physiol.*, **90**, 1119–1124.
4. Carpenter, S. and Karpati, G. (1979) Duchenne muscular dystrophy: plasma membrane loss initiates muscle cell necrosis unless it is repaired. *Brain*, **102**, 147–161.
5. Dalkilic, I. and Kunkel, L.M. (2003) Muscular dystrophies: genes to pathogenesis. *Curr. Opin. Genet. Dev.*, **13**, 231–238.
6. Emery, A.E. (2002) The muscular dystrophies. *Lancet*, **359**, 687–695.
7. Carmeli, E., Moas, M., Reznick, A.Z. and Coleman, R. (2004) Matrix metalloproteinases and skeletal muscle: a brief review. *Muscle Nerve*, **29**, 191–197.
8. Vu, T.H. and Werb, Z. (2000) Matrix metalloproteinases: effectors of development and normal physiology. *Genes Dev.*, **14**, 2123–2133.
9. McCawley, L.J. and Matrisian, L.M. (2001) Matrix metalloproteinases: they're not just for matrix anymore! *Curr. Opin. Cell Biol.*, **13**, 534–540.
10. Miyazaki, D., Nakamura, A., Fukushima, K., Yoshida, K., Takeda, S. and Ikeda, S.I. (2011) Matrix metalloproteinase-2 ablation in dystrophin-deficient mdx muscle reduces angiogenesis resulting in impaired growth of regenerated muscle fibers. *Hum. Mol. Genet.*, **20**, 1787–1799.
11. Hu, J., Van den Steen, P.E., Sang, Q.X. and Opdenakker, G. (2007) Matrix metalloproteinase inhibitors as therapy for inflammatory and vascular diseases. *Nat. Rev. Drug Discov.*, **6**, 480–498.

12. Rullman, E., Rundqvist, H., Wagsater, D., Fischer, H., Eriksson, P., Sundberg, C.J., Jansson, E. and Gustafsson, T. (2007) A single bout of exercise activates matrix metalloproteinase in human skeletal muscle. *J. Appl. Physiol.*, **102**, 2346–2351.
13. Carmeli, E., Moas, M., Lennon, S. and Powers, S.K. (2005) High intensity exercise increases expression of matrix metalloproteinases in fast skeletal muscle fibres. *Exp. Physiol.*, **90**, 613–619.
14. Mackey, A.L., Donnelly, A.E., Turpeenniemi-Hujanen, T. and Roper, H.P. (2004) Skeletal muscle collagen content in humans after high-force eccentric contractions. *J. Appl. Physiol.*, **97**, 197–203.
15. Carvalho, R.F., Dariolli, R., Justulin Junior, L.A., Sugizaki, M.M., Politi Okoshi, M., Cicogna, A.C., Felisbino, S.L. and Dal Pai-Silva, M. (2006) Heart failure alters matrix metalloproteinase gene expression and activity in rat skeletal muscle. *Int. J. Exp. Pathol.*, **87**, 437–443.
16. Fukushima, K., Nakamura, A., Ueda, H., Yuasa, K., Yoshida, K., Takeda, S. and Ikeda, S. (2007) Activation and localization of matrix metalloproteinase-2 and -9 in the skeletal muscle of the muscular dystrophy dog (CXMDJ). *BMC Musculoskelet. Disord.*, **8**, 54.
17. Kherif, S., Dehaupas, M., Lafuma, C., Fardeau, M. and Alameddine, H.S. (1998) Matrix metalloproteinases MMP-2 and MMP-9 in denervated muscle and injured nerve. *Neuropathol. Appl. Neurobiol.*, **24**, 309–319.
18. Kherif, S., Lafuma, C., Dehaupas, M., Lachkar, S., Fournier, J.G., Verdiere-Sahuque, M., Fardeau, M. and Alameddine, H.S. (1999) Expression of matrix metalloproteinases 2 and 9 in regenerating skeletal muscle: a study in experimentally injured and mdx muscles. *Dev. Biol.*, **205**, 158–170.
19. Koskinen, S.O., Kjaer, M., Mohr, T., Sorensen, F.B., Suuronen, T. and Takala, T.E. (2000) Type IV collagen and its degradation in paralyzed human muscle: effect of functional electrical stimulation. *Muscle Nerve*, **23**, 580–589.
20. Reznick, A.Z., Menashe, O., Bar-Shai, M., Coleman, R. and Carmeli, E. (2003) Expression of matrix metalloproteinases, inhibitor, and acid phosphatase in muscles of immobilized hindlimbs of rats. *Muscle Nerve*, **27**, 51–59.
21. Schiotz Thorud, H.M., Stranda, A., Birkeland, J.A., Lunde, P.K., Sjaastad, I., Kolset, S.O., Sejersted, O.M. and Iversen, P.O. (2005) Enhanced matrix metalloproteinase activity in skeletal muscles of rats with congestive heart failure. *Am. J. Physiol. Regul. Integr. Comp. Physiol.*, **289**, R389–R394.
22. Baum, O., Ganster, M., Baumgartner, I., Nieselt, K. and Djonov, V. (2007) Basement membrane remodeling in skeletal muscles of patients with limb ischemia involves regulation of matrix metalloproteinases and tissue inhibitor of matrix metalloproteinases. *J. Vasc. Res.*, **44**, 202–213.
23. Engsig, M.T., Chen, Q.J., Vu, T.H., Pedersen, A.C., Therkidsen, B., Lund, L.R., Henriksen, K., Lenhard, T., Foged, N.T., Werb, Z. *et al.* (2000) Matrix metalloproteinase 9 and vascular endothelial growth factor are essential for osteoclast recruitment into developing long bones. *J. Cell Biol.*, **151**, 879–889.
24. Mott, J.D. and Werb, Z. (2004) Regulation of matrix biology by matrix metalloproteinases. *Curr. Opin. Cell Biol.*, **16**, 558–564.
25. Van Wart, H.E. and Birkedal-Hansen, H. (1990) The cysteine switch: a principle of regulation of metalloproteinase activity with potential applicability to the entire matrix metalloproteinase gene family. *Proc. Natl Acad. Sci. USA*, **87**, 5578–5582.
26. Chen, L.C., Noelken, M.E. and Nagase, H. (1993) Disruption of the cysteine-75 and zinc ion coordination is not sufficient to activate the precursor of human matrix metalloproteinase 3 (stromelysin 1). *Biochemistry*, **32**, 10289–10295.
27. Freimark, B.D., Feeser, W.S. and Rosenfeld, S.A. (1994) Multiple sites of the propeptide region of human stromelysin-1 are required for maintaining a latent form of the enzyme. *J. Biol. Chem.*, **269**, 26982–26987.
28. Park, A.J., Matrisian, L.M., Kells, A.F., Pearson, R., Yuan, Z.Y. and Navre, M. (1991) Mutational analysis of the transin (rat stromelysin) autoinhibitor region demonstrates a role for residues surrounding the "cysteine switch". *J. Biol. Chem.*, **266**, 1584–1590.
29. Fisher, K.E., Fei, Q., Laird, E.R., Stock, J.L., Allen, M.R., Sahagan, B.G. and Strick, C.A. (2002) Engineering autoactivating forms of matrix metalloproteinase-9 and expression of the active enzyme in cultured cells and transgenic mouse brain. *Biochemistry*, **41**, 8289–8297.
30. Michaluk, P., Kolodziej, L., Mioduszewska, B., Wilczynski, G.M., Dzwonek, J., Jaworski, J., Gorecki, D.C., Ottersen, O.P. and Kaczmarek, L. (2007) Beta-dystroglycan as a target for MMP-9, in response to enhanced neuronal activity. *J. Biol. Chem.*, **282**, 16036–16041.
31. Gough, P.J., Gomez, I.G., Wille, P.T. and Raines, E.W. (2006) Macrophage expression of active MMP-9 induces acute plaque disruption in apoE-deficient mice. *J. Clin. Invest.*, **116**, 59–69.
32. Li, H., Mittal, A., Makonchuk, D.Y., Bhatnagar, S. and Kumar, A. (2009) Matrix metalloproteinase-9 inhibition ameliorates pathogenesis and improves skeletal muscle regeneration in muscular dystrophy. *Hum. Mol. Genet.*, **18**, 2584–2598.
33. Charge, S.B. and Rudnicki, M.A. (2004) Cellular and molecular regulation of muscle regeneration. *Physiol. Rev.*, **84**, 209–238.
34. Kuang, S., Kuroda, K., Le Grand, F. and Rudnicki, M.A. (2007) Asymmetric self-renewal and commitment of satellite stem cells in muscle. *Cell*, **129**, 999–1010.
35. Glass, D.J. (2003) Molecular mechanisms modulating muscle mass. *Trends Mol. Med.*, **9**, 344–350.
36. Glass, D.J. (2005) Skeletal muscle hypertrophy and atrophy signaling pathways. *Int. J. Biochem. Cell Biol.*, **37**, 1974–1984.
37. Matsumura, K., Zhong, D., Saito, F., Arai, K., Adachi, K., Kawai, H., Higuchi, I., Nishino, I. and Shimizu, T. (2005) Proteolysis of beta-dystroglycan in muscular diseases. *Neuromuscul. Disord.*, **15**, 336–341.
38. Roma, J., Munell, F., Fargas, A. and Roig, M. (2004) Evolution of pathological changes in the gastrocnemius of the mdx mice correlate with utrophin and beta-dystroglycan expression. *Acta Neuropathol.*, **108**, 443–452.
39. Glass, D.J. (2010) Signaling pathways perturbing muscle mass. *Curr. Opin. Clin. Nutr. Metab. Care*, **13**, 225–229.
40. Ten Broek, R.W., Grefte, S. and Von den Hoff, J.W. (2010) Regulatory factors and cell populations involved in skeletal muscle regeneration. *J. Cell Physiol.*, **224**, 7–16.
41. Lee, S.J., Lee, Y.S., Zimmers, T.A., Soleimani, A., Matzuk, M.M., Tsuchida, K., Cohn, R.D. and Barton, E.R. (2010) Regulation of muscle mass by follistatin and activins. *Mol. Endocrinol.*, **24**, 1998–2008.
42. Bodine, S.C., Stitt, T.N., Gonzalez, M., Kline, W.O., Stover, G.L., Bauerlein, R., Zlotchenko, E., Scrimgeour, A., Lawrence, J.C., Glass, D.J. *et al.* (2001) Akt/mTOR pathway is a crucial regulator of skeletal muscle hypertrophy and can prevent muscle atrophy in vivo. *Nat. Cell Biol.*, **3**, 1014–1019.
43. LeBrasseur, N.K., Walsh, K. and Arany, Z. (2011) Metabolic benefits of resistance training and fast glycolytic skeletal muscle. *Am. J. Physiol. Endocrinol. Metab.*, **300**, E3–E10.
44. Allamand, V. and Campbell, K.P. (2000) Animal models for muscular dystrophy: valuable tools for the development of therapies. *Hum. Mol. Genet.*, **9**, 2459–2467.
45. Stedman, H.H., Sweeney, H.L., Shrager, J.B., Maguire, H.C., Panettieri, R.A., Petrof, B., Narusawa, M., Leferovich, J.M., Sladky, J.T. and Kelly, A.M. (1991) The mdx mouse diaphragm reproduces the degenerative changes of Duchenne muscular dystrophy. *Nature*, **352**, 536–539.
46. Muller, J., Vayssiere, N., Royuela, M., Leger, M.E., Muller, A., Bacou, F., Pons, F., Hugon, G. and Mornet, D. (2001) Comparative evolution of muscular dystrophy in diaphragm, gastrocnemius and masseter muscles from old male mdx mice. *J. Muscle Res. Cell Motil.*, **22**, 133–139.
47. Wehling-Henricks, M., Sokolow, S., Lee, J.J., Myung, K.H., Villalta, S.A. and Tidball, J.G. (2008) Major basic protein-1 promotes fibrosis of dystrophic muscle and attenuates the cellular immune response in muscular dystrophy. *Hum. Mol. Genet.*, **17**, 2280–2292.
48. Wehling, M., Spencer, M.J. and Tidball, J.G. (2001) A nitric oxide synthase transgene ameliorates muscular dystrophy in mdx mice. *J. Cell Biol.*, **155**, 123–131.
49. Acharyya, S., Villalta, S.A., Bakkar, N., Bupha-Intr, T., Janssen, P.M., Carathers, M., Li, Z.W., Beg, A.A., Ghosh, S., Sahenk, Z. *et al.* (2007) Interplay of IKK/NF-kappaB signaling in macrophages and myofibers promotes muscle degeneration in Duchenne muscular dystrophy. *J. Clin. Invest.*, **117**, 889–901.
50. Dogra, C., Changotra, H., Wergedal, J.E. and Kumar, A. (2006) Regulation of phosphatidylinositol 3-kinase (PI3K)/Akt and nuclear factor-kappa B signaling pathways in dystrophin-deficient skeletal muscle in response to mechanical stretch. *J. Cell Physiol.*, **208**, 575–585.
51. Peter, A.K. and Crosbie, R.H. (2006) Hypertrophic response of Duchenne and limb-girdle muscular dystrophies is associated with activation of Akt pathway. *Exp. Cell Res.*, **312**, 2580–2591.
52. Peter, A.K., Ko, C.Y., Kim, M.H., Hsu, N., Ouchi, N., Rhie, S., Izumiya, Y., Zeng, L., Walsh, K. and Crosbie, R.H. (2009) Myogenic Akt signaling

upregulates the utrophin-glycoprotein complex and promotes sarcolemma stability in muscular dystrophy. *Hum. Mol. Genet.*, **18**, 318–327.
53. Mehan, R.S., Greybeck, B.J., Emmons, K., Byrnes, W.C. and Allen, D.L. (2011) Matrix metalloproteinase-9 deficiency results in decreased fiber cross-sectional area and alters fiber type distribution in mouse hindlimb skeletal muscle. *Cells Tissues Organs* [Epub ahead of print, March 9, 2011].
54. Petrella, J.K., Kim, J.S., Cross, J.M., Kosek, D.J. and Bamman, M.M. (2006) Efficacy of myonuclear addition may explain differential myofiber growth among resistance-trained young and older men and women. *Am. J. Physiol. Endocrinol. Metab.*, **291**, E937–E946.
55. Peterson, J.M., Bryner, R.W. and Alway, S.E. (2008) Satellite cell proliferation is reduced in muscles of obese Zucker rats but restored with loading. *Am. J. Physiol. Cell Physiol.*, **295**, C521–C528.
56. Petrella, J.K., Kim, J.S., Mayhew, D.L., Cross, J.M. and Bamman, M.M. (2008) Potent myofiber hypertrophy during resistance training in humans is associated with satellite cell-mediated myonuclear addition: a cluster analysis. *J. Appl. Physiol.*, **104**, 1736–1742.
57. Perry, R.L. and Rudnick, M.A. (2000) Molecular mechanisms regulating myogenic determination and differentiation. *Front Biosci.*, **5**, D750–D767.
58. Lassar, A.B., Buskin, J.N., Lockshon, D., Davis, R.L., Apone, S., Hauschka, S.D. and Weintraub, H. (1989) MyoD is a sequence-specific DNA binding protein requiring a region of myc homology to bind to the muscle creatine kinase enhancer. *Cell*, **58**, 823–831.
59. Wentworth, B.M., Donoghue, M., Engert, J.C., Berglund, E.B. and Rosenthal, N. (1991) Paired MyoD-binding sites regulate myosin light chain gene expression. *Proc. Natl Acad. Sci. USA*, **88**, 1242–1246.
60. Yang, Y., Creer, A., Jemiolo, B. and Trappe, S. (2005) Time course of myogenic and metabolic gene expression in response to acute exercise in human skeletal muscle. *J. Appl. Physiol.*, **98**, 1745–1752.
61. Rommel, C., Bodine, S.C., Clarke, B.A., Rossman, R., Nunez, L., Stitt, T.N., Yancopoulos, G.D. and Glass, D.J. (2001) Mediation of IGF-1-induced skeletal myotube hypertrophy by PI(3)K/Akt/mTOR and PI(3)K/Akt/GSK3 pathways. *Nat. Cell Biol.*, **3**, 1009–1013.
62. Latres, E., Amini, A.R., Amini, A.A., Griffiths, J., Martin, F.J., Wei, Y., Lin, H.C., Yancopoulos, G.D. and Glass, D.J. (2005) Insulin-like growth factor-1 (IGF-1) inversely regulates atrophy-induced genes via the phosphatidylinositol 3-kinase/Akt/mammalian target of rapamycin (PI3K/Akt/mTOR) pathway. *J. Biol. Chem.*, **280**, 2737–2744.
63. Stitt, T.N., Drujan, D., Clarke, B.A., Panaro, F., Timofeyva, Y., Kline, W.O., Gonzalez, M., Yancopoulos, G.D. and Glass, D.J. (2004) The IGF-1/PI3K/Akt pathway prevents expression of muscle atrophy-induced ubiquitin ligases by inhibiting FOXO transcription factors. *Mol. Cell*, **14**, 395–403.
64. Page-McCaw, A., Ewald, A.J. and Werb, Z. (2007) Matrix metalloproteinases and the regulation of tissue remodelling. *Nat. Rev. Mol. Cell Biol.*, **8**, 221–233.
65. Ducharme, A., Frantz, S., Aikawa, M., Rabkin, E., Lindsey, M., Rohde, L.E., Schoen, F.J., Kelly, R.A., Werb, Z., Libby, P. *et al.* (2000) Targeted deletion of matrix metalloproteinase-9 attenuates left ventricular enlargement and collagen accumulation after experimental myocardial infarction. *J. Clin. Invest.*, **106**, 55–62.
66. Cabrera, S., Gaxiola, M., Arreola, J.L., Ramirez, R., Jara, P., D'Armiento, J., Richards, T., Selman, M. and Pardo, A. (2007) Overexpression of MMP9 in macrophages attenuates pulmonary fibrosis induced by bleomycin. *Int. J. Biochem. Cell Biol.*, **39**, 2324–2338.
67. McCroskery, S., Thomas, M., Platt, L., Hennebry, A., Nishimura, T., McLeay, L., Sharma, M. and Kambadur, R. (2005) Improved muscle healing through enhanced regeneration and reduced fibrosis in myostatin-null mice. *J. Cell Sci.*, **118**, 3531–3541.
68. Hnia, K., Hugon, G., Rivier, F., Masmoudi, A., Mercier, J. and Mornet, D. (2007) Modulation of p38 mitogen-activated protein kinase cascade and metalloproteinase activity in diaphragm muscle in response to free radical scavenger administration in dystrophin-deficient Mdx mice. *Am. J. Pathol.*, **170**, 633–643.
69. Nakamura, A., Yoshida, K., Ueda, H., Takeda, S. and Ikeda, S. (2005) Up-regulation of mitogen activated protein kinases in mdx skeletal muscle following chronic treadmill exercise. *Biochim. Biophys. Acta*, **1740**, 326–331.
70. Dogra, C., Changotra, H., Wedhas, N., Qin, X., Wergedal, J.E. and Kumar, A. (2007) TNF-related weak inducer of apoptosis (TWEAK) is a potent skeletal muscle-wasting cytokine. *FASEB J.*, **21**, 1857–1869.
71. Rando, T.A. and Blau, H.M. (1994) Primary mouse myoblast purification, characterization, and transplantation for cell-mediated gene therapy. *J. Cell Biol.*, **125**, 1275–1287.
72. Kuang, S., Charge, S.B., Seale, P., Huh, M. and Rudnicki, M.A. (2006) Distinct roles for Pax7 and Pax3 in adult regenerative myogenesis. *J. Cell Biol.*, **172**, 103–113.
73. Kumar, A., Bhatnagar, S. and Kumar, A. (2010) Matrix metalloproteinase inhibitor batimastat alleviates Pathology and improves skeletal muscle function in dystrophin-deficient mdx mice. *Am. J. Pathol.*, **177**, 248–260.